Polyester/Cellulose Acetate Composites: Preparation, Characterization and Biocompatible

Hui-Min Wang,[1] Yi-Ting Chou,[1] Chin-San Wu,[2] Jen-Taut Yeh[3,4,5]

[1]*Department of Fragrance and Cosmetic Science, Kaohsiung Medical University, Kaohsiung, Taiwan, Republic of China*
[2]*Department of Chemical and Biochemical Engineering, Kao Yuan University, Kaohsiung County, Taiwan, Republic of China*
[3]*Department of Materials Science and Engineering, National Taiwan University of Science and Technology, Taipei, Taiwan*
[4]*Department of Materials Engineering, Kun Shan University, Yung Kang, Tainan, Taiwan, Republic of China*
[5]*Faculty of Chemistry and Material Science, Hubei University, Wuhan, Hubei, China*

Received 11 November 2011; accepted 3 February 2012
DOI 10.1002/app.36965
Published online in Wiley Online Library (wileyonlinelibrary.com).

ABSTRACT: The biocompatibility, morphology, and mechanical thermal properties of composite materials composed of maleic anhydride-grafted polylactide (PLA-*g*-MA) and cellulose acetate (CA) were evaluated. Composites containing maleic anhydride-grafted PLA (PLA-*g*-MA/CA) exhibited noticeably superior mechanical properties due to greater compatibility between the two components. The dispersion of CA in the PLA-*g*-MA matrix was highly homogeneous as a result of ester formation, and the consequent creation of branched and cross-linked macromolecules, between the carboxyl groups of PLA-*g*-MA and hydroxyl groups in CA. The human skin dermal fibroblasts (FBs) seeded on these two novel series membranes to verify the wound dressing characterization properties. With time-dependent course, the FBs proliferation demonstrated a better increasing performance on the series membranes of PLA/CA than PLA-*g*-MA/CA. The immunofluorescent staining illustrated FBs with normal morphological features. The collagen amount from FBs on the PLA/CA series was 25% higher than that seeded on regular culture-plates after 7 days incubation. With CA content from 0 to 20%, the collagen amount increased apparently and up to the position of CA20%. Otherwise, with PLA-*g*-MA membranes, the collagen amount showed moderate stimulations. The SEM image presented secreted collagen from FBs on the PLA/CA membrane, indicating the biofunctional properties of these membranes. The above result analysis, this PLA-*g*-MA/CA composites has good mechanical properties and biocompatible, in the future when use adjusts the formula according to the functionality, may increase the product utility. © 2012 Wiley Periodicals, Inc. J Appl Polym Sci 000: 000–000, 2012

Key words: composites; polyester; human normal dermal fibroblasts; biocompatibility; collagen

INTRODUCTION

There is an increased interest in the production and use of biocompatible polymers all over the world.[1–3] Biocompatible polymers from renewable sources have gained used considerable attention in research and industry due to economic and environmental issues, such as medical application, drug delivery, and waste management and carbon emissions in recent years.[4,5] Aliphatic polyesters have shown great potential in alleviating many of the aforementioned problems.[6] One such membrane, polylactic acid (PLA), can degrade into naturally occurring products in just a few years, as opposed to conventional PLA sticks such as polystyrene (PS) and polyethylene (PE), which require hundreds or even thousands of years to degrade.[7] Unfortunately, PLA is relatively expensive. One way to reduce the cost of PLA composites is by blending them with natural biomaterials. Additionally, there is a continuing need to investigate more environmentally friendly and sustainable materials to PLA-existing materials as industry attempts to lessen the dependence on petroleum-based fuels and products.

Plant fibers that can increase the tensile strength of composites have recently been used as a means of reinforcing polymer matrices as a replacement for synthetic fibers. Cellulose acetate (CA) is an abundant natural fibers resource with excellent tensile strength that can improve the mechanical properties. Therefore, dried CA has been widely applied in thermoplastic composites. Moreover, though CA ranging in length from millimeters to a centimeter and require a compatibilizing agent to wet the fibers,[8,9] the higher hydrophilicity of PLA results in a natural wetting of CA. Composites of PLA and CA thus offer advantages in both mechanical,

Correspondence to: C.-S. Wu (t50008@cc.kyu.edu.tw).

biocompatibility, and cost.[10,11] Furthermore, composites of biodegradable polymers and natural fibers have demonstrated complete degradation in soil or compost without the emission of any toxic or noxious components and have thus received much attention.[12,13]

The skin, the largest organ in the body of vertebrates, is composed of epidermis, dermis, and hypodermis. Fibroblasts (FBs) in dermis are responsible for the body protection from many mechanical and chemical damages, or the injury wound repairing. Cutaneous wound healing, a complicated and highly orchestrated process, is a world-wide issue and a costly procedure for each age range. A number of experimental studies deal with new approaches to improve human skin cell growth using either physical, pharmacological methods, or phyto-therapies.[14,15] Tissue engineering is an effective method for skin wound healing and one of vital aims of cell biologists was to stimulate cell growth using sophisticated environmental conditions. In this research, these membranes are aimed to be used on wound dressing.[16] Wound dressings prevent loss of body fluid and exudate buildup, to protect the wounds from external contamination, to have sufficient bactericidal effects to inhibit infection and to simulate a friendly microenvironment for cells to proliferate.[17]

Collagen is an essential constituent and major compartment of human connective tissues, especially in skin soft tissues and is a major structural protein of ECM, supporting the growth of a wide variety of tissue.[18] Collagen is a natural substrate of the extracellular matrix, and in wound healing, it would guide FBs and attract fibrogenic cells which help in wound healing. It was reported that high collagen content would be expected to promote cell attachment due to integrin binding with cell adhesion domains in collagen. Besides, in the presence of certain neutral salt molecules, collagen can act as a nucleating agent causing fibrillar structure formation. In the process of wound healing, blood platelets also interact with the collagen to make a hemostatic plug.[19,20]

This report described a systematic investigation of the mechanical properties and biocompatibility of CA composites with PLA and maleic anhydride-grafted PLA. The composites were characterized using Fourier-transform infrared spectroscopy (FTIR) and ^{13}C nuclear magnetic resonance (NMR) to identify bulk structural changes induced by the maleic anhydride moiety. Additionally, the effects of CA content on biocompatibility and cell proliferation rate of human dermal FBs on these membranes were evaluated for wound dressing appropriate properties. Furthermore, the production of such green composites would concurrently lessen the dependence on synthetic fibers and reduce the amount of wasted CA.

EXPERIMENTAL PART

Materials

Maleic anhydride (MA), benzoyl peroxide (BPO), PKH-67, Sirius Red dye, and dimethyl sulfoxide (DMSO), were purchased from Sigma-Aldrich Chemical (St. Louis, MO). The polylactide was supplied by Nature Works (Nebraska, USA), and was composed of 95% L-lactide and 5% meso-lactide with a weight average molecular weight (M_w) of 9.75×10^4, a number average molecular weight (M_n) of 5.07×10^4, a polydispersity index of 1.92, and a melt-flow index of 18.5 g/10 min. MA was purified before use by recrystallization from chloroform. Benzoyl peroxide (BPO; Sigma) was used as an initiator, and was purified by dissolution in chloroform and reprecipitation in methanol. 3-[4,5-dimethylthiazo$_l$-2-yl]-5-[3-carboxymethoxyphenyl]-2-[4-sulfophenyl]-2*H*-tetrazolium, inner salt (MTS) from Promega (Madison, WI). Fetal bovine serum (FBS) and Dulbecco's modified Eagle's medium (DMEM) were obtained from Gibco BRL (Gaithersburg, MD). All buffers and other reagents were of the highest purity commercially available. CA (3.5 g, degree of deacetylation 55%), supplied by Showa Chemical (Tokyo, Japan), was dissolved in 31.5 g of acetone to increase its dispersion in the polymer matrix and avoid aggregation.

Prepare and test of PLA-Cellulose Acetate membranes

PLA-*g*-MA copolymer

Under a nitrogen atmosphere and at 60 ± 2°C, maleic anhydride was grafted onto PLA being dissolved in xylene solution, and the polymerization reaction was initiated with BPO. The reaction system was stirred at 60 rpm for 6 h. The grafted product (4g) was then dissolved in 200 mL refluxing xylene at 60 ± 2°C and the hot solution was filtered through several layers of cheesecloth. The cheesecloth was washed with acetone to remove the tetrahydrofuran-insoluble unreacted maleic anhydride and the product remained over the cheesecloth was then dried in a vacuum oven at 80°Cfor 24 h. The xylene-soluble product in the filtrate was extracted five times, using 600 mL cold acetone for each extraction operation. Subsequently, the grafting percentage was determined, using a titration method.[21] The titration showed a grafting percentage of about 1.13 wt %. BPO and MA loading were maintained at 0.3 and 10 wt %, respectively.

Composite preparation

The mass ratios of CA to PLA or PLA-*g*-MA were fixed at 5/95, 10/90, 15/85, and 20/80, and

composites were prepared using a "plastograph" 200 Nm mixer W50EHT instrument (Brabender, Hackensack, NJ) with a blade-type rotor; the rotor speed was maintained at 50 rpm and the temperature at 160°C, with a reaction time of 25 min. Next, the composites were pressed into 1-mm-thick plates using a hot press at 160°C, and then placed in a desiccator for cooling. The cooled plates were then made into standard samples for characterization.

Characterization analyses

The composites were characterized using Fourier-transform infrared spectroscopy (FTIR) and ^{13}C nuclear magnetic resonance (NMR) to identify bulk structural changes induced by the maleic anhydride moiety. Solid-state ^{13}C NMR was performed using an AMX-400 NMR spectrometer (Bruker Billerica, Bremen, Germany) and was obtained at 100 MHz under cross-polarization while spinning at the magic angle. Power decoupling conditions were set with a 90° pulse and a 4-s cycle time. Infrared spectra of the samples were obtained using an FTS-7PC FTIR spectrophotometer (Bio-Rad, Hercules, CA), using thin films, was used to investigate the graft reaction of maleic anhydride onto PLA and to verify the incorporation of the modified CA to the extent that bonds were formed in the hybrids. An Instron mechanical tester (Model LLOYD, LR5K type, Segensworth, Fareham, UK) was used to measure the tensile strength and the elongation at break in accordance with ASTM D638. Test samples were prepared in a hydrolytic press at 140°C and conditioned at 50 ± 5% relative humidity for 24 h before making measurements. Measurements were made using a cross-head speed of 20 mm/min. Five measurements were performed for each sample and the mean value was determined. Morphology of composites was recorded using a scanning electron microscope (Hitachi Microscopy Model S-1400, Japan). Before coating with gold, the samples from the mechanical analysis were first treated with hot water at 80°C for 24 h to rinse out possibly detained impurities. Afterward, residual water on the samples was removed via suction in vacuum at 80°C for 2 h. The glass transition temperature (T_g), melt temperature (T_m), and fusion heat (ΔH_f) were determined using a TA Instrument 2010 DSC system (New Castle, DE). The DSC was calibrated using the melting temperature and enthalpy of indium. DSC sample films were sealed in aluminum pans (amounts ranged from 4 to 6 mg) under N_2 atmosphere, while melting curves were recorded from a low of −30°C to a high of +200°C at a rate of 10°C/min.

Bio-functions of human normal dermal FBs on PLA series membranes

Human dermal FB cell cultures

The primary cultures of human skin FBs were isolated from foreskin primary culture, which were obtained from Chung-Ho Memorial Hospital, Kaohsiung Medical University, Taiwan (KMUH-IRB-990269). FBs were incubated at 37°C in a humidified incubator 5% CO_2 atmosphere.[22] To seed the cells on the membranes, the authors cut the membranes to the shape and well size of 48 well plates, sterilized with ethanol, and UV light and before seeding, the membranes were rinsed with DMEM medium. For each membrane in the well, 5×10^4 cells were seeded. To study the cytotoxicities of human skin cells on these membranes, the authors used MTS assay.[23] 1, 4, and 7 days after cells were seeded on the membranes, the cells in 100 μL medium were exposed to 20 μL of CellTiter 96 AQueous One Solution (Promega, USA), for 3 h according to the manufacturers' instructions. Absorbance at 490 nm was recorded using a spectrometer plate reader (UV-Vis, BioTek, USA).

PKH-67 labeling

Human dermal FBs on the membranes were stained PKH-67 (a green fluorescent compound that incorporated aliphatic reporter molecules into the cell membrane by selective partitioning, Sigma-Aldrich, USA) to be observed with fluorescence. Cells were incubated with 5 μ*M* PKH-67 for 5 min at 25°C and gently vortexed every 30 s (according to the manufacturer's protocol). Unincorporated PKH-67 was removed by washing the cells with complete medium. PKH-67 labeled cells were re-seeded on the testing membranes at a density of 1×10^5/μl, and then fluorescent images were taken.

Collagen quantification

For measurement of total collagen amount secreted by FBs on the membranes, Sirius Red dye was used to stain total collagen.[24] The authors compared the collagen secreted by FBs incubated on 48 well plates or on different membranes. After indicated time interval, mediums were removed and cells washed with PBS twice. 100 μL of 0.1% Sirius Red stain (0.05 g Sirius red powder per 50 mL picric acid) was added to each well and kept at room temperature for 1 h. The unattached stain was removed and washed for five times with 200 μL of 0.1 *N* HCl. After removing the unattached stain, images of the samples were taken under the microscope to observe collagen distribution. The attached stain was extracted with 100 μL of 0.1 *N* NaOH (15 min) and

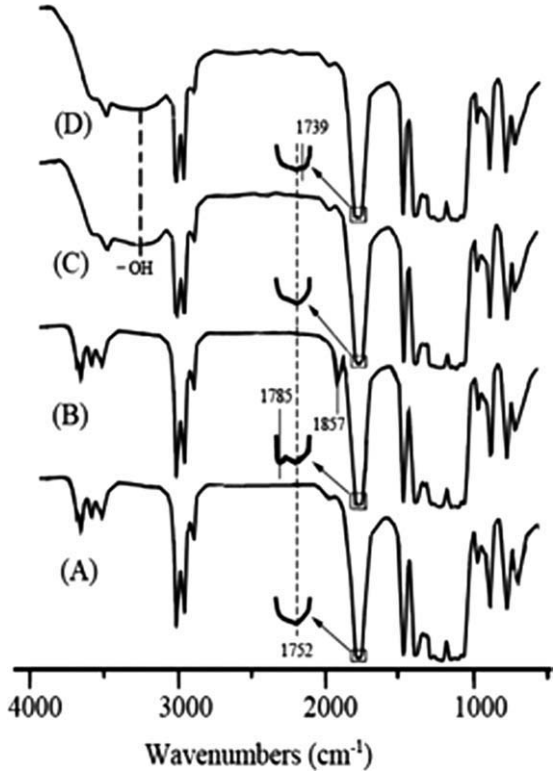

Figure 1 FTIR spectra for (A) PLA, (B) PLA-*g*-MA, (C) PLA/CA (10 wt %), and (D) PLA-*g*-MA/CA (10 wt %).

mixed well. The stain was placed into 96 well plates to read the absorbance at 540 nm using a spectrometer plate reader. By quantifying the collagen amount of the scaffold without cell seeding and deducting the OD value, the collagen/HA/gelatin scaffold background was excluded.

Statistical analysis

Results are presented as a mean value of the data obtained from triplicate experiments. Student's *t*-test was used to determine the level of significance. Differences were considered nonsignificant when $P > 0.05$, significant when $P \leq 0.05$, and very significant when $P \leq 0.01$.

RESULTS AND DISCUSSION

FTIR/NMR analyses

The FTIR spectra of unmodified PLA and PLA-*g*-MA are shown in Figure 1(A and B), respectively. The characteristic transitions of PLA[25] at 3300 $\sim$ 3700, 1700 $\sim$ 1760, and 500 $\sim$ 1500 cm^{-1} appeared in the spectra of both polymers, with two extra shoulders observed at 1785 and 1857 cm^{-1} in the modified PLA spectrum. These features are characteristic of anhydride carboxyl groups. Similar results have been reported earlier.[26] The shoulders represent free acid in the modified polymer and therefore denote the grafting of MA onto PLA.

In the composite PLA/CA (10 wt %), the peak assigned to the O–H stretching vibration at 3200 $\sim$ 3700 cm^{-1} intensified [Fig. 1(C] due to contributions from the –OH group of CA. The FTIR spectrum of the PLA-*g*-MA /CA (10 wt %) composite in Figure 1(D) revealed a peak at 1739 cm^{-1} that was not present in the FTIR spectrum of the PLA/CA (10 wt %) blend. This peak was assigned to the ester carbonyl stretching vibration of the copolymer. Wu also reported an absorption peak at 1739 cm^{-1} for this ester carbonyl group.[27] By the above result, when after CA and PLA-*g*-MA prepared composite, the Figure 1(B) absorption peak 1785 and 1857 cm^{-1} shift to 1739 cm^{-1}. This data suggest because the formation of branched and cross-linked macromolecules in PLA-*g*-MA/CA by covalent reaction of the anhydride carboxyl groups in PLA-*g*-MA with the hydroxyl groups of CA.

To further confirm this conclusion, solid-state ^{13}C NMR spectra of PLA and PLA-*g*-MA are compared in Figure 2(A and B), respectively. There are three

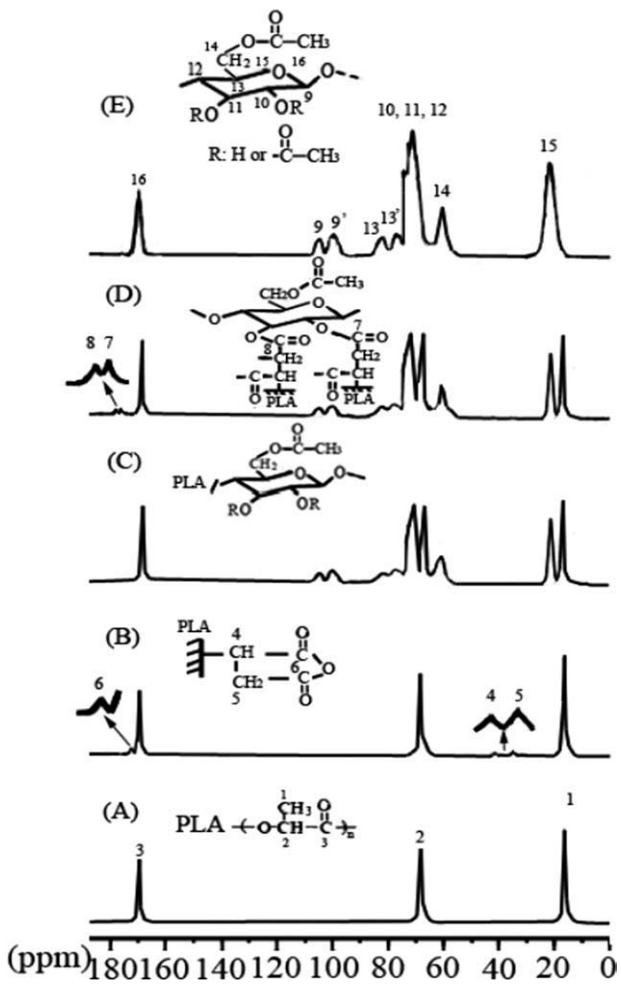

Figure 2 Solid-state ^{13}C NMR spectra for (A) PLA, (B) PLA-*g*-MA, (C) PLA/CA (10 wt %), (D) PLA-*g*-MA/CA (10 wt %), and (E) CA.

peaks corresponding to carbon atoms in the unmodified PLA (1: δ = 16.93 ppm; 2: δ = 68.76 ppm; 3: δ = 169.92 ppm). Wu reported a similar finding in a new biodegradable blends prepared from polylactide and hyaluronic acid.[28] The ^{13}C NMR spectrum of PLA-*g*-MA showed additional peaks (4: δ = 42.25 ppm; 5: δ = 35.92 ppm; 6: δC=O δ = 172.86 ppm), thus confirming that MA was covalently grafted onto PLA.

The solid-state ^{13}C NMR spectra of PLA-*g*-MA/CA (10 wt %), PLA/CA (10 wt %), and CA are shown in Figure 2(C) through Figure 2(E). There are three peaks corresponding to carbon atoms in the pure CA in Figure 2(E). The spectra are similar to those reported by Lima et al.[29] Relative to unmodified PLA, additional peaks were observed in the spectra of composites containing PLA-*g*-MA. These additional peaks were located at δ = 42.25 ppm (4) and δ = 35.92 ppm (5). These same features were observed in earlier studies[30] and indicate grafting of MA onto PLA. However, the peak at δ = 172.86 ppm (C = O) (6) [shown in Fig. 2(B)], which is also typical for MA grafted onto PLA, was absent in the solid-state spectrum of PLA-*g*-MA/CA (10 wt %). This is most likely a result of an additional condensation reaction between the anhydride carboxyl group of MA and the –OH group of CA that caused the peak at δ = 172.86 ppm to split into two bands (δ = 174.96 and 176.66 ppm). This additional reaction converted the fully acylated groups in the original CA to esters [represented by peaks 8 and 9 in Fig. 2(C)] and did not occur between PLA and CA, as indicated by the absence of corresponding peaks in the FTIR spectrum of PLA/CA (10 wt %) in Figure 2(D). The formation of ester groups significantly affects the mechanical properties properties of PLA-*g*-MA/CA and is discussed in greater detail in the following sections.

Composite morphology

In most composite materials, effective wetting and uniform dispersion of all components in a given matrix, and strong interfacial adhesion between the phases are required to obtain a composite with satisfactory mechanical properties. In the current study, CA may be thought of as a dispersed phase within a PLA or- PLA-*g*-MA matrix. To evaluate the composite morphology, SEM was used to examine tensile fractures in the surfaces of PLA/CA (10 wt %) and PLA-*g*-MA/CA (10 wt %) samples. The SEM microphotograph of PLA/CA (10 wt %) in Figure 3(A) shows that the CA fibers in this composite tended to poor interfacial adhesion in the matrix. This poor interfacial adhesion was due to the formation of hydrogen bonds between CA and the disparate hydrophilicities of PLA and CA. Poor wetting in these composites was also noted [Fig. 3(A)] due to large differences in surface energy between the CA and the PLA matrix.[31]

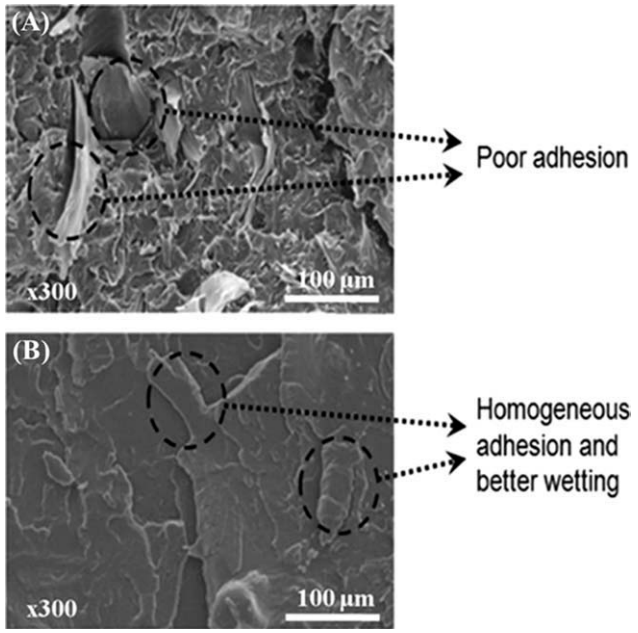

Figure 3 SEM photomicrographs show the distribution and adhesion of CA in (A) PLA/CA (10 wt %) and (B) PLA-*g*-MA/CA (10 wt %) composites.

In contrast, the PLA-*g*-MA/CA (10 wt %) microphotograph presented in Figure 3(B) shows a more homogeneous dispersion and better wetting of CA in the PLA-*g*-MA matrix, as indicated by the complete coverage of PLA-*g*-MA on the fiber and the removal of both materials when a fiber was pulled from the bulk. This improved interfacial adhesion is due to the similar hydrophilicity of the two components, which allows for the formation of branched and cross-linked macromolecules, and the prevention of hydrogen bonding between CA fibers.

Mechanical properties

Figure 4 shows the variation in tensile strength at break with CA content for PLA/CA and PLA-*g*-MA/CA composites. The tensile strength of neat PLA decreased when it was grafted with maleic anhydride. This may be due to in the blends, CA will expand PLA or PLA-*g*-MA, hence causing slack polymer structure and reduced tensile strength. For PLA/CA composites (dotted line in Fig. 4), tensile strength at break decreased markedly and continuously as the CA content increased. This is due to the poor dispersion of CA in the PLA matrix and demonstrates that incompatibility between the two polymers has a significant impact on the mechanical properties of the composite. This was attributed to poor dispersion of CA in the PLA matrix, as discussed previously and as shown in Figure 3(A). The tensile strength of PLA-*g*-MA/CA (solid line in

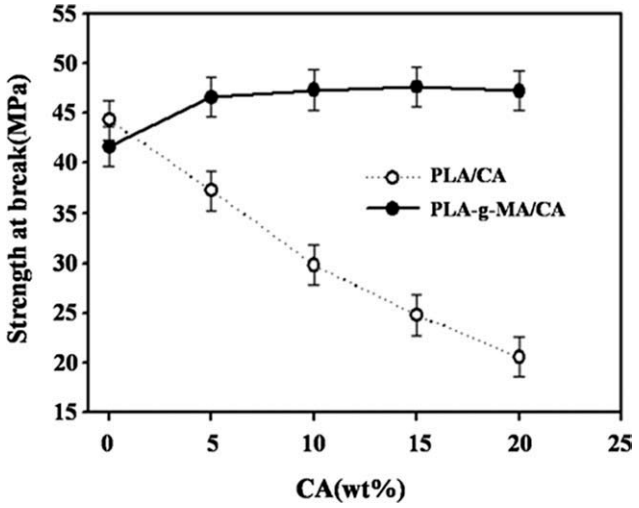

Figure 4 The effect of CA content on tensile strength at break is shown for PLA/CA and PLA-*g*-MA /CA composites.

Fig. 4) is lower than that of PLA. Tensile strength increased at 10 wt % CA due to esterification between PLA-*g*-MA and CA. The tensile strength decreased at high levels of CA due to agglomeration and uneven distribution of residual CA, which was present due to the low grafting rate of 1.13%. Furthermore, it was found that the PLA-*g*-MA/CA composites not only gave larger values of tensile strength than the PLA/CA composites but also they yielded more stable tensile strengths when the CA content was above 10 wt %. This may be, in part, due to the more homogeneous dispersion resulting from the formation of branched or cross-linked macromolecules of CA in the PLA-*g*-MA matrix. Grafting of the MA onto PLA increased the tensile strength of the CA composite.

Differential scanning calorimetry

The heat of fusion ΔH_f) and melt temperatures (T_m) of both PLA/CA and PLA-*g*-MA/CA blends with various CA content were determined by measuring DSC heating thermograms (shown in Table I). For both blends, T_m decreased with increasing CA content. This may be due to in the blends, CA will expand PLA or PLA-*g*-MA, hence causing slack polymer structure and reduced T_m. At the same CA content, the PLA/CA blend had a higher T_m than the PLA-*g*-MA/CA blend. The glass transition temperature (T_g) increased with increasing CA content for both PLA/CA and PLA-*g*-MA/CA blends. This increase was likely a result of decreasing space available for molecular motion. T_g values were higher for the PLA-*g*-MA composite by between 0.5 and 5.0°C, suggesting that the grafting of anhydride carboxyl groups to the PLA further restricted molecular motion.

The ΔH_f of pure PLA was 36.5 J/g, whereas that of PLA-*g*-MA was 34.1 J/g (Table I). The lower ΔH_f of PLA-*g*-MA was likely due to the disruption of regularity in chain structure and increased spacing between chains as a result of the grafted branches. The values of ΔH_f in PLA-*g*-MA/CA were approximately 2–12 J/g higher than those of PLA/CA. These higher ΔH_f values were likely due to the formation of ester carbonyl groups as discussed above. The ΔH_f may be used as an indicator of blend crystallinity. Although ΔH_f of both PLA/CA and PLA-*g*-MA/CA blends decreased with increased CA content (Table I), the extent of the decrease was significantly greater in PLA/CA, indicating a lower degree of crystalline. These results are similar to those obtained with blends of PLA and natural fibers.[32] The marked decrease in the crystallinity of PLA/CA was most likely due to hindered motion of the PLA polymer segments as a result of the presence of CA in the composite matrix.[33]

Cell proliferation

To assure the biocompatibility and cell growth rate of human normal skin, dermal FBs seeded on the membranes were studied (Fig. 5). The cell morphology on these membranes was observed under microscope and the cell viability was examined by MTS assay. To detect the skin cell distribution, the authors used PKH67 to stain the cells before seeding on the membranes [Fig. 5(A–I)]. From the fluorescent photos under microscope, it showed the cell morphology on these membranes were quite similar to the control. Human dermal FBs were normally distributed over membranes which the membranes were proved to be appropriate for cell growth. The FBs cell numbers on different membranes were measured [Fig. 5(J)]. With FBs seeding on the membranes, the PLA-CA series membranes showed similar cell viabilities to FBs seeded on the plate directly from 1st day to 7th day, which revealed that the membranes have good compatibility to human dermal FBs. With more CA content, the cell viability does not show obvious difference, with CA content

TABLE I
Effect of CA Content on the Thermal Properties of PLA/CA and PLA-*g*-MA/CA Composites

	PLA/CA			PLA-*g*-MA/CA		
CA (wt %)	T_g (°C)	T_m (°C)	ΔH_f (J/g)	T_g (°C)	T_m (°C)	ΔH_f (J/g)
0	57.3	161.4	36.5	57.8	158.8	34.1
5	58.0	158.9	28.4	62.1	155.9	32.9
10	59.1	157.8	25.3	64.1	152.6	32.2
15	59.9	157.4	23.4	65.4	152.3	31.7
20	60.6	157.1	21.0	65.7	152.1	31.2

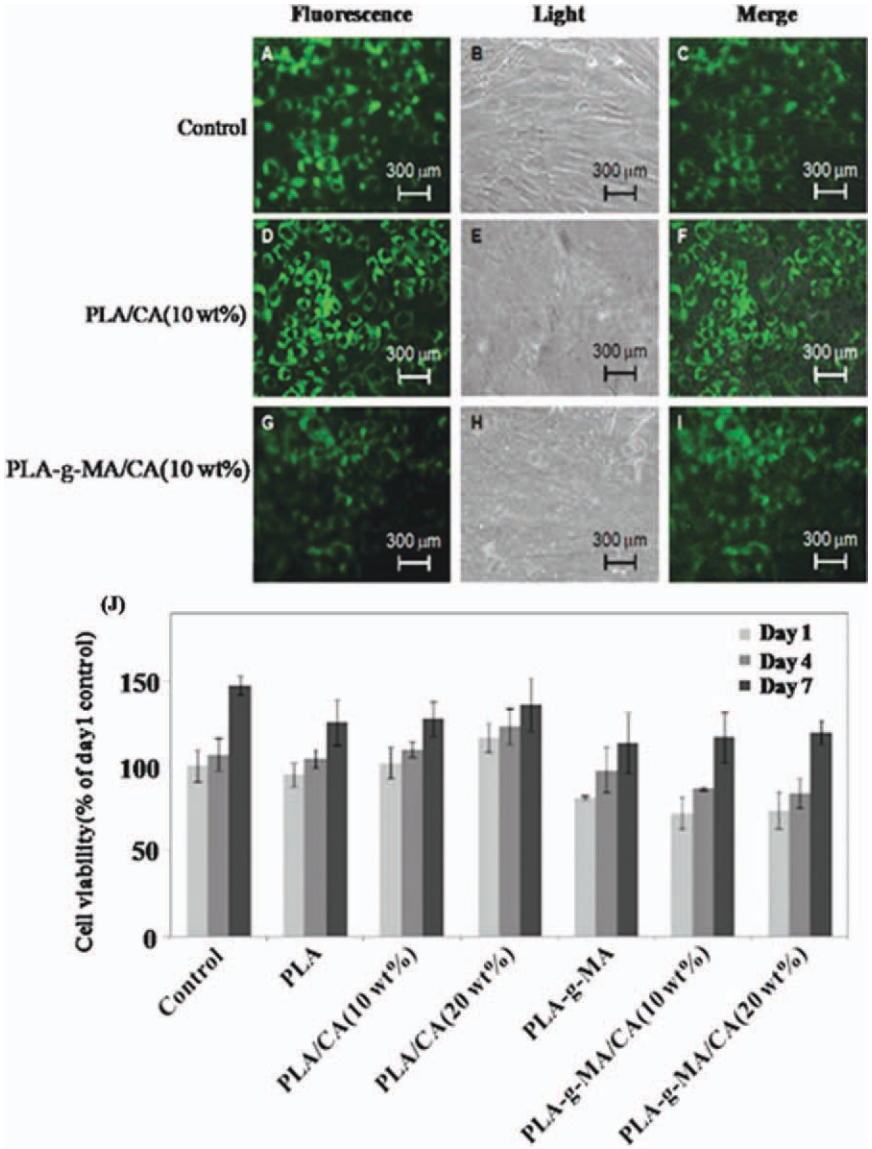

Figure 5 Photographed and cell proliferation ratios of human skin FBs seeded on two series membranes. PKH-67 was used to stain cells (A, D, and G); bright field (B, E, and H); merged phase (C, F, and I) (scale bar is 300 μm). From 1 to 7 days, the cell proliferation rate was quantified by MTS assay (J). [Color figure can be viewed in the online issue, which is available at wileyonlinelibrary.com.]

of 5 and 15%, the results were alike (data not shown). The FBs cell viabilities on PLA-*g*-MA membranes were slightly lower than on the plate at the 1st day. On the 7th day, though, the cell viabilities were quite similar to the PLA-CA series and on the plate. The cell viabilities of cells on PLA-*g*-MA series membranes slightly lower than on PLA/CA series membranes might be due to the slight toxicity of MA.

Collagen amount

Sirius Red dye was used to stain the collagen secreted by dermal FBs on the well or on the membranes. In Figure 6, comparing to seeding FBs on the plates, the collagen productions on different membranes were similar at day 1. At day 4 or 7, collagen productions by dermal FBs on PLA-CA were obvious higher than on the plate, the vehicle control. Among the PLA-CA membranes, the collagen production increased with more CA contents, Amid the PLA-*g*-MA series, the collagen amount is less than PLA series but also more than the control at the 4th day. At day 7, the collagen amount on PLA series membranes showed obvious increase. It showed that PLA series membranes stimulated the collagen secretion of FBs. While seeding on PLA-*g*-MA series membranes for 7 days, the collagen secretion of FBs did not show noticeable enhancements and this might be the cytotoxicity of MA.

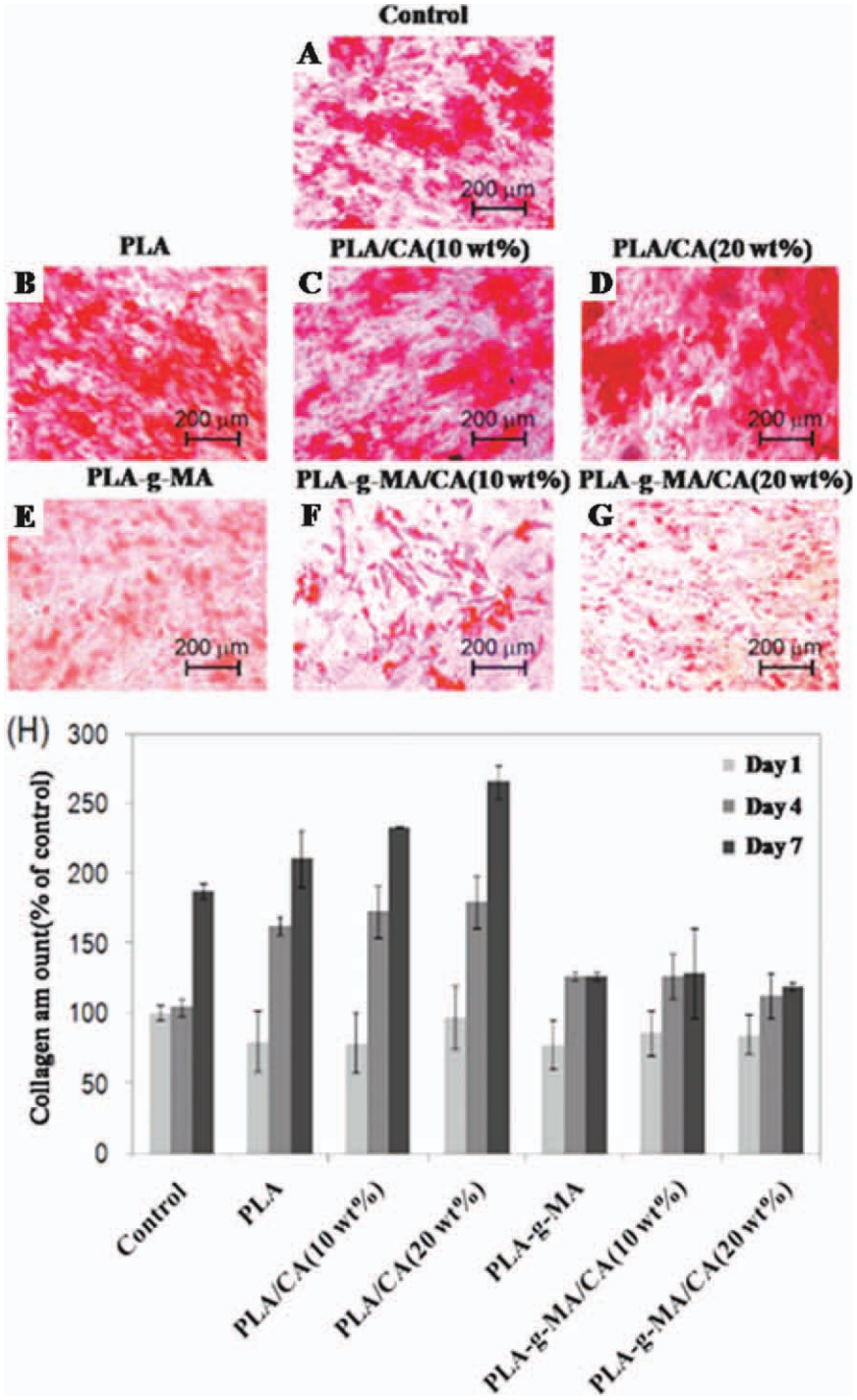

Figure 6 Photographed and collagen amount secreted from FBs seeded on two series membranes for 7 days. Sirius Red dye was used to stain collagen (A–G; scale bar is 200 μm); quantification of the collagen amount (H). [Color figure can be viewed in the online issue, which is available at wileyonlinelibrary.com.]

Collagen is an important component for cell proliferation and tissue body formation which are dependent on FBs production.[34] Collagen in ECM imparts appropriate mechanical strength to the tissue body shape.[35,36] Therefore, in skin wound healing promotion, to detect the concentration of the collagen secreted amount is a key index. Since the PLA series membranes stimulated collagen secretion by FBs, these may be good biomaterials for tissue engineering on wound dressing. Figure 7(A–F) showed the SEM image of collagen and FBs on cell-treatment membranes (7 days). The arrows indicated the thread-like collagen. The SEM demonstrated compacted fibril morphology of collagen, comparing to Figure 6. With more CA contents in PLA, on the SEM photos more excretion were observed, this

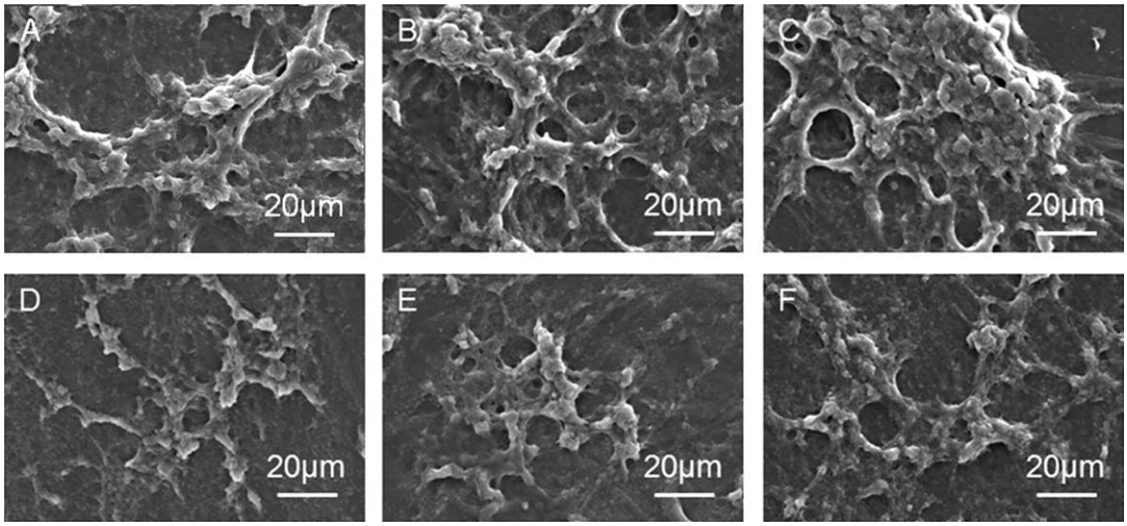

Figure 7 The SEM image of FBs and collagen on the (A) PLA, (B) PLA/CA (10 wt %), (C) PLA/CA (20 wt %), (D) PLA-*g*-MA, (E) PLA-*g*-MA/CA (10 wt %), and (F) PLA-*g*-MA /CA (20 wt %) membranes after 7 days culture (scale bar is 20 μm). The arrows indicated the fibril-like collagen.

attested the collagen quantification data that the membranes could stimulate collagen production.

CONCLUSION

The biocompatibility and mechanical properties of CA blended with PLA and maleic anhydride-grafted recycled PLA were examined. FTIR and NMR analyses revealed the formation of ester groups from reactions between -OH groups in SF and carboxyl groups in PLA-*g*-MA, significantly altering the structure of the composite materials. The morphology of the PLA-*g*-MA/CA composites was consistent with good adhesion between the CA phase and the PLA-*g*-MA matrix. In mechanical tests, MA grafting enhanced the mechanical properties of the composite, especially the tensile strength. The cell viability tests indicated that PLA membranes have good biocompatibility for FBs to proliferate upon. These membranes could accelerate the healing progress by promoting FBs collagen productions. The collagen secretion by FBs stimulated by PLA series membranes indicated the potential for PLA/CA membranes on wound dressings.

The author thanks the National Science Council (Taipei City, Taiwan, R.O.C.) for financial supports (NSC-99-2221-E-037-006-MY3 and NSC 99-2622-E-244-001-CC3).

References

1. Chae, S. Y.; Kim, H. J.; Lee, M. S.; Jang, Y. L.; Lee, Y.; Lee, S. H.; Lee, K.; Kim, S. H.; Kim, H. T.; Chi, S.-C.; Park, T. G.; Jeong, J. H. Macromolecules 2011, 44, 848.
2. Bellocq, C.; Kang, D. W.; Wang, X.; Jensen, G. S.; Pun, S. H.; Schluep, T.; Zepeda, M. L.;.Davis, M. E. Bioconjugate Chem 2004, 15, 1201.
3. Irfan, M.; Seiler, M. Ind Eng Chem Res 2010, 49, 1169.
4. Davis, G.; Song, J. H. Ind Crop Prod 2006, 23, 147.
5. Vilaplana, F.; Strömberg, E.; Karlsson, S. Polym Degrad Stab 2010, 95, 2147.
6. Raquez, J.-M.; Deléglise, M.; Lacrampe, M.-F.; Krawczak, P. Prog Polym Sci 2010, 35, 487.
7. Wang, K.-H.; Wu, T.-M.; Shih, Y.-F.; Huang, C.-M. Polym Eng.Sci 2008, 48, 1833.
8. Moad, G. Prog Polym Sci 2011, 36, 218.
9. Edgar, K. J.; Buchanan, C. M.; Debenham, J. S.; Rundquist, P. A.; Seiler, B. D.; Shelton, M. C.; Tindall, D. Prog Polym Sci 2001, 26, 1605.
10. Anderson, J. M.; Shive, M. S. Adv Drug Deliv Rev 1997, 28, 5.
11. Malafaya, P. B.; Silva, G. A.; Reis, R. L. Adv Drug Deliv Rev 2007, 59, 207.
12. Nalawade, S. P.; Picchioni, F.; Janssen, L. P. B. M. Prog Polym Sci 2006, 31, 19.
13. Noel, M.; Fredon, E.; Mougel, E.; Masson, D.; Masson, E.; Delmotte, L. J. Bioresour Technol 2009, 100, 4711.
14. Dainiak, M. B.; Allan, I. U.; Savina, I. N.; Cornelio, L.; James, E. S.; James, S. L.; Mikhalovsky, S. V; Jungvid, H.; Galaev, I. Y. Biomaterials 2010, 31, 67.
15. Tripathi, A.; Kathuria, N.; Kumar, A. J Biomed Mater Res A 2009, 90, 680.
16. Corin, K. A.; Gibson, L. J. Biomaterials 2010, 31, 4835.
17. Volety, A. K.; Oliver, L. M.; Genthner, F. J.; Fisher, W. S. Aquaculture 1999, 172, 205.
18. Duan, X.; Sheardown, H. J Biomed Mater Res A 2005, 75, 510.
19. Broos, K.; Feys, H. B.; De Meyer, S. F.; Vanhoorelbeke, K.; Deckmyn, H. Blood Rev 2011, 25, 155.
20. Shanmugam, M.; Kumar, T. S.; Arun, K. V.; Arun, R.; Karthik, S. J. J Indian Soc Periodontol 2010, 14, 241.
21. Wu, C. S. Polym Degrad Stab 2009, 94, 1076.
22. Wang, H. M.; Chen, C. Y.; Ho, M. L.; Chou, Y. T.; Chang, H. C.; Lee, C. H.; Wang, C. Z.; Chu, I. M. Bioorg Med Chem 2010, 18, 5241.
23. Han, J.; Ma, I.; Hendzel, M. J.; Allalunis-Turner, J. Breast Cancer Res 2009, 11, R57.

24. Walsh, B. J.; Thornton, S. C.; Penny, R.; Breit, S. N. Anal Biochem 1992, 203, 187.
25. Yang, S.-I.; Wu, Z-H.; Yang, W.; Yang, M. -B. Polym Test 2008, 27, 957.
26. Nakason, C.; Kaesaman, A.; Supasanthitikul, P. Polym Test 2004, 23, 35.
27. Wu, C. S. Polym Degrad Stab 2003, 80, 127.
28. Wu, C. S. Polymer 2005, 46, 10017.
29. Lima, G. M.; Sierakowski, M.-R.; Faria-Tischer, P. C. S.; Tischer, C. A. Mater Sci Eng C 2011, 31, 190.
30. Marshall, G. L.; Wilson, S. J. Eur Polym J 1988, 24, 939.
31. Wong, K. J.; Zahi, S.; Low, K. O.; Lim, C. C. Mater Des 2010, 31, 4147.
32. Wang, K.-H.; Wu, T.-M.; Shih, Y.-F.; Huang, C.-M. Polym Eng Sci 2008, 48, 1833.
33. Wu, C. S. J Appl Polym Sci 2003, 89, 2888.
34. Orlandi, A.; Ferlosio, A.; Gabbiani, G.; Spagnoli, L. G.; Ehrlich, P. H.; Exp Cell Res 2005, 311, 317.
35. Ruszczak, Z. Adv Drug Deliv Rev 2003, 55, 1595.
36. Sell, S. A.; McClure, M. J.; Garg, K.; Wolfe, P. S.; Bowlin, G. L. Adv Drug Deliv Rev 2009, 61, 1007.